Charge Pumping of Interacting Fermion Atoms in the Synthetic Dimension

Tian-Sheng Zeng,[1] Ce Wang,[2] and Hui Zhai[2]
[1]School of Physics, Peking University, Beijing 100871, China
[2]Institute for Advanced Study, Tsinghua University, Beijing 100084, China
(Received 14 April 2015; published 28 August 2015)

Recently it has been theoretically proposed and experimentally demonstrated that a spin-orbit coupled multicomponent gas in a 1D lattice can be viewed as a spinless gas in a synthetic 2D lattice with a magnetic flux. In this Letter we consider interaction effects in such a Fermi gas, and propose these effects can be easily detected in a charge pumping experiment. Using 1/3 filling of the lowest 2D band as an example, in the strongly interacting regime, we show that the charge pumping value gradually approaches a universal fractional value for large spin components and low filling of the 1D lattice, indicating a fractional quantum Hall-type behavior, while the charge pumping value is zero if the 1D lattice filling is commensurate, indicating a Mott insulator behavior. The charge-density-wave order is also discussed.

DOI: 10.1103/PhysRevLett.115.095302 PACS numbers: 67.85.Lm, 03.75.Ss, 67.85.Fg, 67.85.Hj

High spin quantum gas is a unique system of cold atom physics. For instance, alkali atoms like Rb and Na have hyperfine spin $F = 1$, and a K atom has $F = 9/2$, a lanthanide atom such as Dy has $J = 8$, and alkali-earth-(like) atoms such as Yb and Sr have a large nuclear spin with $SU(W)$ symmetry, where W can be as large as ~ 10. Recently, an interesting idea has emerged to use the internal spin degrees of freedom as another dimension, named as the "synthetic dimension," which naturally extends a D-dimensional system into a $(D+1)$-dimensional one [1,2]. In a 1D lattice system, by applying two counter-propagating Raman beams to couple different spin states, one can create a magnetic flux lattice in synthetic 2D geometry [2]. This proposal requires a minimum amount of laser light and therefore minimizes heating from spontaneous emission. It also gives rise to a sharp edge in the synthetic dimension, which can help to visualize edge states. Very recently, two experimental groups have implemented this scheme, in a Rb atom [3] and in a Yb atom [4], respectively, and chiral edge states have been observed, for noninteracting (or weakly interacting) bosons [3] and fermions [4], respectively. Moreover, it is also possible to create more exotic nontrivial geometries [5].

The experimental setup and basic idea of the synthetic dimension are briefly illustrated in Fig. 1. For instance, two Raman beams with π and σ polarizations couple spin state $|m\rangle$ to $|m \pm 1\rangle$, where m can take any value between $-F$ and F with a total of $W = 2F + 1$ components. The Raman coupling has a spatial dependent phase factor $e^{i2k_R x}$, where k_R is the recoil momentum of Raman laser. Here we introduce γ as $\gamma = 2k_R a = 2\pi/q$ (a is lattice spacing), and the single particle Hamiltonian is therefore written as

$$\hat{H}_0 = \sum_{j,m} (-t\hat{c}^\dagger_{j+1,m}\hat{c}_{j,m} + \Omega e^{-i\gamma j}\hat{c}^\dagger_{j,m-1}\hat{c}_{j,m} + \text{H.c.}), \quad (1)$$

where j labels the site along the physical dimension $\hat{x}$ and m labels internal spin components. t is the hopping amplitude along $\hat{x}$ and Ω is the Raman coupling strength. There are two different but equivalent views of this single-particle Hamiltonian.

(a) A 1D system of high spin atoms with spin-orbit coupling: by applying a spin and site dependent rotation $\hat{c}_{j,m} \to e^{i\gamma jm}\hat{c}_{j,m}$, the Hamiltonian Eq. (1) becomes

$$\hat{H}_0 = \sum_{j,m} (-te^{-i\gamma m}\hat{c}^\dagger_{j+1,m}\hat{c}_{j,m} + \Omega\hat{c}^\dagger_{j,m-1}\hat{c}_{j,m} + \text{H.c.}) \quad (2)$$

The spin dependent hopping term, together with a constant spin flipping term, gives rise to the spin-orbit coupling effect, which has been extensively discussed in the continuum case in the past few years [6–10].

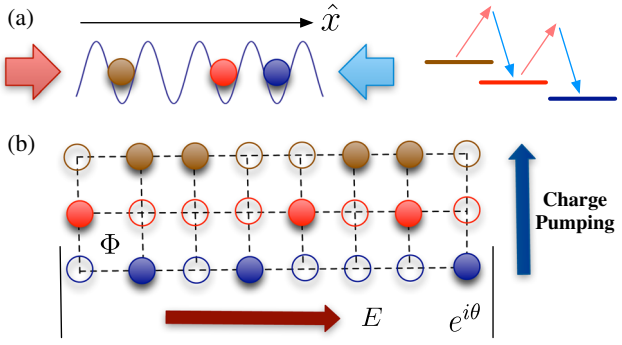

FIG. 1 (color online). Illustration of two different physical pictures of this system and the idea of charge pumping. (a) Two Raman beams along $\hat{x}$ are applied to a multicomponent quantum gas in optical lattices. The Raman beams couple different spin states and generate a coupling between spin and momentum k_x. (b) Different spin components are viewed as another dimension, and the system is mapped into a 2D spinless particle in a magnetic field. By applying an electric field along the physical dimension $\hat{x}$, it generates a charge pumping along the synthetic dimension, which can be detected by measuring spin populations.

(b) A 2D system with magnetic flux: If we view m as another synthetic dimension, say, labeled by $\hat{y}$, Eq. (1) represents a situation that spinless atoms hop in a 2D space, with a finite number (W) of chains and an open boundary condition along $\hat{y}$. More importantly, hopping along a close loop around a plaquette accumulates a phase of γ, that is equivalent to say, each plaquette has a flux of Φ_0/q (Φ_0 is magnetic flux unit).

These two equivalent views build up an intriguing connection between spin-orbit coupled high spin particles in 1D and spinless but charged particles in a 2D ladder geometry with magnetic flux. For instance, at the single-particle level, the chiral edge current from scenario (b), as observed in Refs. [3,4], is equivalent to the spin-momentum locking effect from scenario (a), as observed in the spin-1/2 case [6–8]. In this Letter we aim at studying the effect of repulsive interaction in this system [11]. For 2D electron gas in a magnetic field, it is known that the fractional quantum Hall (FQH) state will emerge with strong repulsive interactions. However, in this system there are a few important differences that are worth emphasizing first.

(1) In the synthetic dimension, the system always only has a finite number of chains. Though it is possible to create a periodic boundary condition in the synthetic dimension with a certain complicated laser setting, in the most simple and natural setup, the system has an open boundary condition in the synthetic dimension. Thus, the finite size effect can be significant.

(2) Along the physical dimension, the interaction is on site and short-ranged. While in the synthetic dimension, the interaction is long-ranged. Let us consider a $SU(W)$ invariant interaction [12],

$$\hat{H}_{\text{int}} = U \sum_{j,m\neq m'} \hat{n}_{j,m}\hat{n}_{j,m'}, \tag{3}$$

atoms in any two sites along the synthetic dimension, despite of their separation, interact with the same interaction strength. In another words, in the 2D lattice the interaction is very anisotropic.

(3) For a normal FQH effect, the only relevant parameter ν is the ratio between fermion number to flux number. In our case, it will be

$$\nu = \frac{N}{N_{\text{flux}}} = \frac{N}{WL/q} = \frac{Nq}{WL}, \tag{4}$$

where N is the total number of fermions, L is the number of sites along the $\hat{x}$ direction. However, from the picture (a) that our system is one dimensional, it is natural to introduce another filling factor,

$$\nu_{1\text{D}} = \frac{N}{L}, \tag{5}$$

and if $\nu_{1\text{D}}$ is an integer, one may expect a trivial Mott insulator rather than a FQH state when interaction U is sufficiently large. Thus, when ν is fixed, we still have two other tunable parameters, i.e., $\nu_{1\text{D}}$ and W.

Hereafter we shall fix $\nu = 1/3$ as a typical example. Given the differences mentioned above, one may wonder whether one will still have a FQH-type behavior under strong repulsive interactions. Besides, whether there is an effective scheme to detect such a state in this cold atom setting. The rest of this Letter is devoted to answering this question.

Charge pumping.—To reveal the interaction effect, we propose to perform a charge pumping experiment utilizing the advantage of the synthetic dimension. Let us consider applying an electric field along the $\hat{x}$ direction. In a cold atom experiment, this can be realized by a moving lattice with a constant velocity v or by applying a field gradient for a short period of time to shift momentum by θ/L. For a moving lattice, in the comoving frame a constant vector potential mv appears as required in charge pumping argument [13], which also corresponds to a periodic boundary condition with $\theta = mvL$. In our numerical calculation below, this is implemented by a twisted boundary condition in the $\hat{x}$ direction, i.e., $\Psi(L) = e^{i\theta}\Psi(0)$. Charge pumping here means charge transfer along the synthetic dimension [13], as schematized in Fig. 1. Defining the "charge polarization per unit length" as

$$Y = \frac{1}{W}\sum_{j,m}\langle\hat{n}_{j,m}\rangle m, \tag{6}$$

the charge transfer along the synthetic dimension after inserting one flux is given by

$$Q = Y(\theta = 2\pi) - Y(\theta = 0). \tag{7}$$

Following discussions in the previous literature [14], this value is quantized in the limit of large W for a topological band [15]. If it is in real space, detecting charge transfer requires an *in situ* image, while charge transfer in the synthetic dimension means the changing of the spin population, which can be easily detected from the Stern-Gerlach experiment in the time-of-flight image [16,17].

In Fig. 2, we present the charge pumping value Q for various $\nu_{1\text{D}}$ and W, with ν fixed at $1/3$. This result is obtained by numerically solving the many-body wave functions with Hamiltonian $\hat{H} = \hat{H}_0 + \hat{H}_{\text{int}}$, either by exact diagonalization (ED) or density matrix renormalization group (DMRG) methods. For ED the maximum number of particles is six and the dimension of Hilbert space is of the order of 3×10^7. For DMRG, the maximum number of particles is ten, and the truncation error is of the order of 10^{-7}. Each eigenstate has a well-defined quantum number K that is the center-of-mass momentum along $\hat{x}$. We also plot how these eigenstates evolve under the changing of θ, as shown in Fig. 3, and for the ground state, we calculate Y as a function of θ with Eq. (6) and deduce Q with Eq. (7).

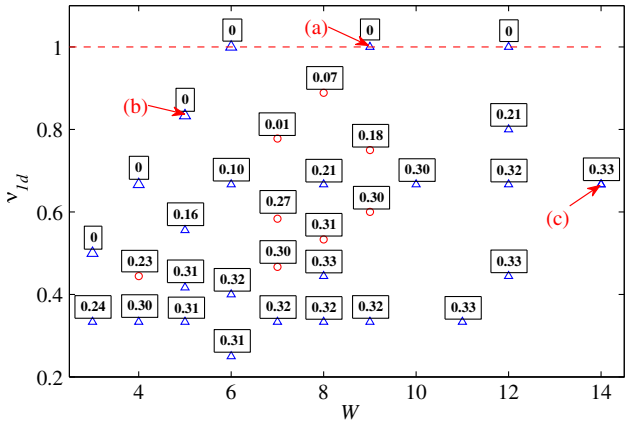

FIG. 2 (color online). Charge pumping for different ν_{1D} and W. The numbers in the boxes are charge pumping Q after insertion of one flux [15]. Blue triangles are points calculated by ED and red circles are points calculated by DMRG, with ν fixed at $1/3$, $\Omega = t$ and $U = 6t$. (a)–(c) Three marked cases where spectral flow will be shown in Fig. 3.

We find the following features in Fig. 2. (i) For $\nu_{1D} = 1$, Q is identically zero for all W. In this case there is always a unique ground state which will not interchange with other states under flux insertion, as shown in Fig. 3(a). This is a Mott insulator phase with commensurate ν_{1D}. (ii) Since here we consider q as an integer, the smallest value for q is $q = 2$. With $q = 2$ and $\nu = 1/3$, $\nu_{1D} = \nu W/q$ can at most be $W/6$. We note that for $q = 2$, the Hofstadter spectrum exhibits a Dirac cone instead of a fully gapped band, and the lowest band does not have a well-defined Chern-number. Therefore, for $\nu_{1D} = W/6$ (with $W \leq 6$) we also find $Q = 0$. A typical spectral flow and charge pumping is shown in Fig. 3(b). (iii) For small W, or for larger W but ν_{1D} closer to unity, though Q is generally nonzero, it takes a nonuniversal value. This fluctuating Q indicates some Fermi-liquid type states [18]. (iv) For large W and small ν_{1D}, Q gradually approaches a universal fractional value of $1/3$. A typical spectral flow under flux insertion is shown in Fig. 3(c). One can see that three low-lying states (though not exactly degenerate) exchange one with the other as θ increases, and the spectrum recovers itself only after θ changes 6π. These features are consistent with a FQH effect. This is because for large W, the finite size effect in the synthetic dimension becomes insignificant, and for smaller ν_{1D} away from commensurate filling, the lattice effect also becomes weaker. For intermediate W, the value is not exactly $1/3$ partially due to the finite size effect in the definition of Y in Eq. (6). Previously, it has been shown by the Luttinger liquid theory that for continuum models, a fractional state can emerge in a one-dimensional system with spin-orbit coupling [19].

We also study the charge pumping value Q as a function of Raman coupling strength Ω, as shown in Fig. 4. As the synthetic magnetic field results from Raman coupling, one naturally expects that Q will vanish as $\Omega \to 0$. Indeed, we

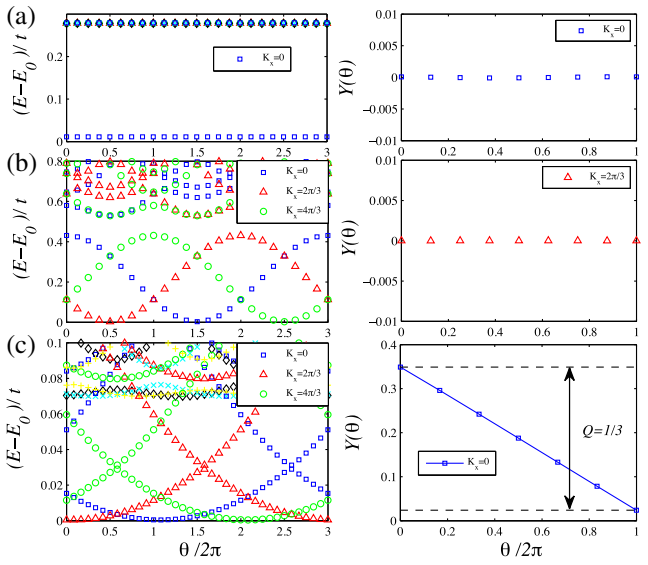

FIG. 3 (color online). Left column: Spectral flow under the insertion of flux (i.e., changing periodic boundary condition θ from zero to 6π.) Right column: Charge polarization Y as a function of θ. (a)–(c) correspond to different W and ν_{1D} as marked in Fig. 2. (a) $W = 9$, $\nu_{1D} = 1$ ($N = L = 5$), $q = 3$; (b) $W = 5$, $\nu_{1D} = 5/6$ ($N = 5$, $L = 6$), $q = 2$, and (c) $W = 14$, $\nu_{1D} = 2/3$ ($N = 4$, $L = 6$), $q = 7$. All of these cases are calculated by ED. $U = 6t$ and $\Omega = t$.

show in Fig. 4 that when Ω/t is smaller than a certain value, Q starts to deviate from $1/3$ and drops fast to zero. This feature is particularly clear for large W (e.g., green points for $W = 14$ in Fig. 4). We have also looked at Q for smaller U/t and found when $U < t$, Q also takes a fluctuating nonuniversal value.

Periodic boundary conditions in the synthetic dimension.—We also find that if one applies a more involved laser setting to achieve a periodic boundary condition along the synthetic dimension, it will help to stabilize the topological degeneracy of a fractional state. For instance, for the cases with $W = 4$ we presented in Fig. 2, we do not find accurate fractional charge pumping. While when we apply a

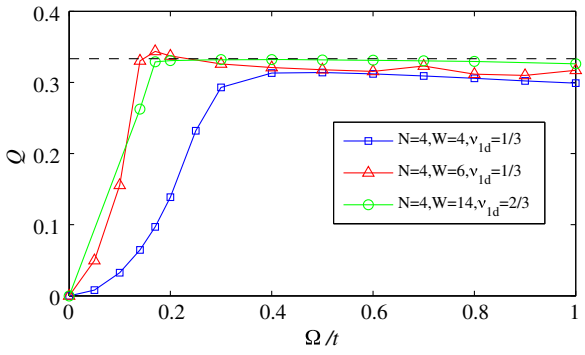

FIG. 4 (color online). Charge pumping Q as a function of Raman coupling strength Ω/t. The dashed line is $1/3$. Here $U = 6t$ and other parameters are shown in the legend.

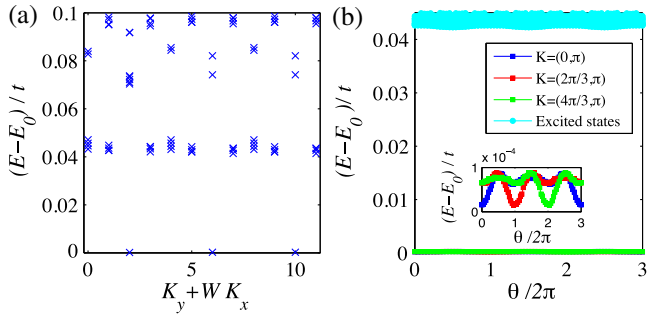

FIG. 5 (color online). Energy diagram with periodic boundary condition in the synthetic dimension. (a) Energy levels for different momenta $K_y + WK_x$. (b) Energy of the lowest three states as a function of θ. Here $W = 4$, $\nu_{1D} = 1/3$ ($N = 4$, $L = 12$), $q = 4$. This case is also calculated by ED. $U = 6t$ and $\Omega = t$.

periodic boundary condition in the synthetic dimension, we show the energy level for different momenta (labeled by $K_y + WK_x$ as now both K_x and K_y are good quantum numbers) in Fig. 5, and we find a very accurate threefold degeneracy, with an energy splitting smaller than $10^{-4}t$, and these states are separated from other excited states by a gap $\sim 0.04t$. The total momentums of these three states are also consistent with generalized Pauli-exclusion principle analysis [20]. Moreover, these states exchange one another under the flux insertion, and do not intersect with other excited states, as shown in Fig. 5(b). By calculating the Berry curvature with twisted boundary conditions in both physical and synthetic dimensions [18], we numerically find that their many-body Chern numbers $\mathcal{C}_1 = \mathcal{C}_2 = \mathcal{C}_3 = 0.333$.

Density order.—Finally we look at real-space charge density order. We consider the on site total density $\rho_j = \sum_m \langle \hat{n}_{j,m} \rangle$. In Fig. 6, we plot the Fourier transform of ρ_i as $\rho(q_x) = (1/L)\sum_j (\rho_j - \bar{\rho}) e^{iq_x j}$ ($\bar{\rho} = \nu_{1D}$ is the average density). $\rho(q_x)$ shows a clear peak at $q_x/(2\pi) = \nu_{1D}$ and $q_x/(2\pi) = 1 - \nu_{1D}$. This feature exists for both open and periodic boundary conditions along the synthetic

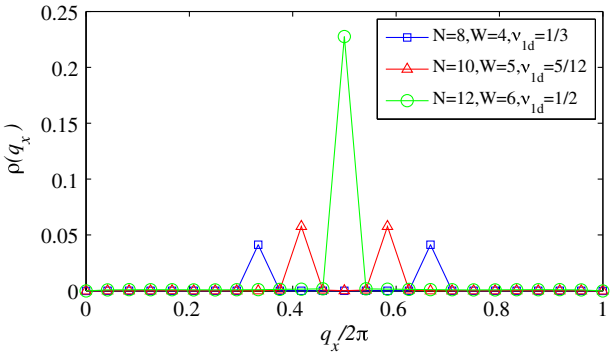

FIG. 6 (color online). Fourier transformation of density $\rho(q_x)$ for different values of W and ν_{1D}. $U = 6t$, $\Omega = t$ and other parameters are shown in the legend.

dimension. A similar situation has also been found in several other models [21]. This is reminiscent of the usual FQH state in the thin torus limit [22].

Conclusion.—In summary, we have studied interaction effects in the synthetic dimension picture of high spin lattice Fermi gases with Raman-coupling induced spin-orbit coupling. Our studies are mainly focused on the charge pumping experiment, which becomes much easier in this setting, as the charge pumping along the synthetic dimension can be visualized by measuring the spin population. For the fixed $\nu = 1/3$ case, we investigate how the charge pumping value depends on the number of spin component W, fermion density ν_{1D}, and Raman coupling Ω/t. We conclude that a universal fractional charge pumping $Q = 1/3$ is favorable for $W \gg 1$, $\nu_{1D} \ll 1$, $\Omega/t \sim 1$, and with strong interactions. We also remark that the experimental imperfections, such as finite temperature effect and particle density fluctuation, will all cause derivation from this universal value. However, the quantitative features shown in Fig. 2 are still robust. Nevertheless, in order to observe the exact quantized value one has to cool the system below the gap ($\sim 0.04t$) and use a flat-bottom trap to precisely control density. Similar results have also been obtained for strongly interacting bosons.

We would like to thank Hong Yao for helpful discussion. This work is supported by Tsinghua University Initiative Scientific Research Program (H. Z.), NSFC Grants No. 11174176 (H. Z.), No. 11325418 (H. Z.), No. 11274022 (T. S. Z.) and NKBRSFC under Grant No. 2011CB921500 (H. Z.).

Note added.—Recently, we become aware of another paper, Ref. [23], in which the same system is studied by DMRG. Charge density wave order is also discussed in this paper.

[1] O. Boada, A. Celi, J. I. Latorre, and M. Lewenstein, Phys. Rev. Lett. **108**, 133001 (2012).
[2] A. Celi, P. Massignan, J. Ruseckas, N. Goldman, I. B. Spielman, G. Juzeliunas, and M. Lewenstein, Phys. Rev. Lett. **112**, 043001 (2014).
[3] B. K. Stuhl, H.-I Lu, L. M. Aycock, D. Genkina, and I. B. Spielman, arXiv:1502.02496.
[4] M. Mancini, G. Pagano, G. Cappellini, L. Livi, M. Rider, J. Catani, C. Sias, P. Zoller, M. Inguscio, M. Dalmonte, and L. Fallani, arXiv:1502.02495.
[5] O. Boada, A. Celi, M. Lewenstein, J.Rodrguez-Laguna, and J. I. Latorre, New J. Phys. **17**, 045007 (2015).
[6] Y.-J. Lin, K. Jimnez-Garca, and I. B. Spielman, Nature (London) **471**, 83 (2011).
[7] P. Wang, Z. Q. Yu, Z. Fu, J. Miao, L. Huang, S. Chai, H. Zhai, and J. Zhang, Phys. Rev. Lett. **109**, 095301 (2012).
[8] L. W. Cheuk, A. T. Sommer, Z. Hadzibabic, T. Yefsah, W. S. Bakr, and M. W. Zwierlein, Phys. Rev. Lett. **109**, 095302 (2012).

[9] H. Zhai, Int. J. Mod. Phys. B **26**, 1230001 (2012); V. Galitski and I. B. Spielman, Nature (London) **494**, 49 (2013); H. Zhai, Rep. Prog. Phys. **78**, 026001 (2015).

[10] Studying spin-orbit coupling for high spin atoms has also been proposed in X. Cui, B. Lian, T. L. Ho, B. L. Lev, and H. Zhai, Phys. Rev. A **88**, 011601(R) (2013).

[11] A paper appeared recently studying few-body problems with attractive interaction in this geometry: S. K. Ghosh, U. K. Yadav, and V. B. Shenoy, arXiv:1503.02301.

[12] For the alkali-earth atom, the interaction is $SU(W)$ invariant. For the alkali atom, this is also a very good approximation since the spin-dependent interaction is usually quite small and the spin mixing collision takes place in a much longer time scale than the time scale for the synthetic magnetic field and $SU(W)$ invariant part of density interaction.

[13] D. J. Thouless, Phys. Rev. B **27**, 6083 (1983).

[14] R. D. King-Smith and D. Vanderbilt, Phys. Rev. B **47**, 1651 (1993); G. Ortiz and R. M. Martin, Phys. Rev. B **49**, 14202 (1994); N. Marzari, A. A. Mostofi, J. R. Yates, I. Souza, and D. Vanderbilt, Rev. Mod. Phys. **84**, 1419 (2012); X.-L. Qi, Phys. Rev. Lett. **107**, 126803 (2011); M. Barkeshli and X.-L. Qi, Phys. Rev. X **2**, 031013 (2012); S. Coh and D. Vanderbilt, Phys. Rev. Lett. **102**, 107603 (2009); L. Wang, M. Troyer, and X. Dai, Phys. Rev. Lett. **111**, 026802 (2013).

[15] See Supplemental Material at http://link.aps.org/supplemental/10.1103/PhysRevLett.115.095302 for (i) explanation of the definition of "charge polarization per unit length" for a topological band;and (ii) details of parameters for each point in Fig. 2, such as spin components W, total fermion number N, system length L, flux q ($\Phi = \Phi_0/q$).

[16] Another type of charge pumping, that is, applying a current in the synthetic dimension and detecting charge pumping in the physical dimension, was also proposed in a recent paper: N. R. Cooper and A. M. Rey, arXiv:1503.05498 [Journal (to be published)].

[17] In fact, a simple version of this kind of "charge pumping" has been observed in a dipole oscillation experiment of a BEC: J. Y. Zhang, S. C. Ji, Z. Chen, L. Zhang, Z. D. Du, Bo Yan, G. S. Pan, B. Zhao, Y. J. Deng, H. Zhai, S. Chen, and J. W. Pan, Phys. Rev. Lett. **109**, 115301 (2012). When atoms move with finite velocity during dipole oscillation, spin transfer from one component to another component has also been observed.

[18] D. N. Sheng, Z. C. Gu, K. Sun, and L. Sheng, Nat Comm **2**, 389 (2011).

[19] C. L. Kane, R. Mukhopadhyay, and T. C. Lubensky, Phys. Rev. Lett. **88**, 036401 (2002); and Y. Oreg, E. Sela, and A. Stern, Phys. Rev. B **89**, 115402 (2014).

[20] N. Regnault and B. A. Bernevig, Phys. Rev. X **1**, 021014 (2011).

[21] B. A. Bernevig and N. Regnault, arXiv:1204.5682; Z. Xu, L. Li, and S. Chen, Phys. Rev. Lett. **110**, 215301 (2013); F. Grusdt and M. Honing, Phys. Rev. A **90**, 053623 (2014); T. S. Zeng and L. Yin, Phys. Rev. B **91**, 075102 (2015).

[22] A. Seidel, H. Fu, D. H. Lee, J. M. Leinaas, and J. Moore, Phys. Rev. Lett. **95**, 266405 (2005).

[23] S. Barbarino, L. Taddia, D. Rossini, L. Mazza, and R. Fazio, arXiv:1504.00164.